PRP Pharmacology Research & Perspectives
Open Access

ORIGINAL ARTICLE

Microparticle of drug and nanoparticle: a biosynthetic route

Sounik Sarkar & Anjan Kr. Dasgupta

Department of Biochemistry and Centre of Excellence in Biomedical Engineering and Systems Biology, University of Calcutta, 35 Ballygunge Circular Road, Kolkata 700019, India

Keywords
Doxorubicin, drug delivery, microparticle, nanoparticle, platelet

Correspondence
Anjan Kr. Dasgupta, Department of Biochemistry and Centre of Excellence in Biomedical Engineering and Systems Biology, University of Calcutta, 35 Ballygunge Circular Road, Kolkata 700019, India.
Tel: +919748758663;
Fax: +913324614849;
E-mail: adgcal@gmail.com

Funding Information
Indian Council of Medical Research (ICMR) (Grant/Award Number: '45/06/2011/NAN-BMS').

Received: 5 June 2015; Revised: 11 August 2015; Accepted: 18 August 2015

Pharma Res Per, 3 (5), 2015, e00188, doi: 10.1002/prp2.188

doi: 10.1002/prp2.188

Abstract

Microparticles (MPs) have great potentiality in material science- based applications. Their use in biology is however limited to clinics and has rarely been exploited in the pharmaceutical context. Unlike nanoparticles (NPs), they are amenable to routine detection by flow cytometry and confocal microscopy. Though MPs can constitute a wide variety of materials, including ceramics, glass, polymers, and metals and can be synthesized by chemical process but wet processes for the preparation of microparticles have rarely been attemped. In this paper, a thrombotic route is shown to successfully generate biocompatible MP of a model anticancer drug (doxorubicin hydrochloride). Synthesis of MPs from platelets and drug loading in to these MPs was confirmed by flow cytometry and confocal microscopy. Human cervical cancer cell line (HeLa) was treated with these drug-loaded MPs to investigate whether the loaded MPs have the capacity to deliver drug to the cancer cells. In addition, Magnetic force microscopy was used to detect the preparation of MPs loaded with magnetic NPs. The efficiency of the drug-loaded MPs in inducing cytotoxicity in cancer cell line, shown to be significantly higher than the free drug itself. The drug-loaded MP is shown to have a much higher cytotoxic propensity than the free drug applied at comparable doses. The thrombotic approach can also be applied to synthesize MP containing NPs which in turn can lead to generate a wide variety of new biocompatible materials.

Abbreviations

Dox, doxorubicin hydrochloride; MOD, microparticle of drug; MON, microparticle of nanoparticle; MP, microparticle; PMP, platelet-derived microparticle; PRP, platelet-rich plasma; WP, washed platelet.

Introduction

Over the past decade, the massive interest for research lies in the field of nanomaterials due to their potential applications in the field of industrial, biomedical, and electronics (Dastjerdi and Montazer 2010; Ramachandraiah et al. 2015). The nanomedicine perspectives for the use of nanoparticles (NPs) are largely devoted to synthesize nanoforms with minimal toxicity issues particularly in context with drug delivery (Kahaleh et al. 2008; Matyjasik-Liggett and Wittman 2013). In many cases, the nanosize or even the nanosurface becomes less important than the conjugant which the nanoform is supposed to carry and deliver in a targeted fashion. An advantage in the microscale domain lies in the fact that unlike NPs, microparticles (MPs) which are comparable to the cellular size (order of microns) have lesser tendency to form clusters into the intracellular domains (Copple et al. 2008; Kang et al. 2008).

The cellular uptake mechanism in the nanoscale (typically of the size of a globular protein) may differ entirely from the mechanism by which the MPs enter into the cell (Rejman et al. 2004). Unlike their nanocounterparts, miroparticles can be subjected to analysis by microscopy, or flow cytometry and many other conventional techniques. Further, easy separation methods with more stringent control over size and shape make MPs a suitable candidate in various applications including pharmaceutical preparations (Padalkar et al. 2011).

Till date several methods have been employed to prepare MPs, like conventional emulsion-based methods, polymerization techniques, Spray drying, solvent extraction, phase separation coacervation technique etc (Lee et al. 1999; Mu and Feng 2001; Yeo et al. 2001; Jyothi et al. 2010). To use these MPs in the field of pharmaceuticals different approaches have been made to change the surface properties of these microparticulate materials to protect them against phagocytic clearance and make them biocompatible. Several methods have also been employed to load active components into the MPs. Among these, two methods are very common for loading of active components into these MPs, firstly during the time of preparation of MP and after formation of the MPs by incubating drug/desired materials with them (Alagusundaram et al. 2009). Apart from the biomedical applications in microscopy or flow cytometry, other avenues where self-assembly of MP may be exploited include induction-controlled inter-particle spacing which in turn is useful in wide range of applications, including making a sensing device, microfluidic templates and other material science-based applications (Cook et al. 2001; Chandler et al. 2011).

Though numerous wet processes for the preparation of nanoparticles are known, wet processes for the preparation of microparticles are uncommon. As a result, most of the MPs known today are made up of routine materials such as glass, special polymers (e.g., polystyrene), with magnetic or fluorescent coatings (Guo et al. 2006). Accordingly, there exists a need for a biological or chemical wet process that allows the use of diversified materials for the preparation of microparticles with various desirable attributes.

In biological process, various cell types release small membrane-bound vesicles ranging between 0.1 and 1 μm (Enjeti and Seldon 2012; Schindler et al. 2014). These cell-derived micron range particles, sheded by an active process, lack a nucleus and may contain cytoskeletal proteins, DNA or RNA. To date, the cell types reported to release MPs either constitutively or when stimulated include platelets, blood cells, endothelium, epithelium, and various cancer cells (Davila et al. 2008; Bastarache et al. 2009; Burnier et al. 2009). Among these, platelet-derived microparticles (PMPs) are the most widely studied and consist of the majority of the MP population in blood (Horstman and Ahn 1999; Berckmans et al. 2001; Joop et al. 2001). Previously considered as cell debris they are now regarded as vectors for transfer of biological information (Enjeti and Seldon 2012). Like their parental cells, PMPs can also stimulate proliferation and adhesion of cancer cells (Cocucci et al. 2009; Varon and Shai 2009).

In the present study, we choose platelets as a MP synthesizing precursor and will represent a technique to synthesize drug and NP-loaded MPs by using a natural property of platelets namely releasing of MPs upon activation. Till date no such report has been found to synthesize biocompatible MPs loaded with desired materials by following a simple biological route. The technique that we have evolved for the preparation of MPs, enables easily loading of drugs or tiny nanoforms in it and have coined them MOD (Microparticle of Drug) and MON (Microparticle of Nanoparticles) for drug-loaded MP and NP-loaded MP, respectively. As derived from platelets, their biocompatibility will be unquestionable and thus may have tremendous possible application in drug delivery to bio- imaging, as a whole in the pharmaceuticals industry.

Materials and Methods

Platelet preparation

Blood was collected from normal volunteers with permission of the Institutional Ethical Committee (No. 29 dated 7 May 2014) and the informed written consent was taken from the individual prior to testing. A total of 9 mL of blood was mixed in 1 mL of 3.2% sodium citrate anticoagulant (final ratio 9:1 whole blood/citrate). Platelet-rich plasma (PRP) was obtained after centrifuging blood at 200 *g* for 12 min. Platelet poor plasma (PPP) was obtained by centrifugation of blood at 1500 *g* for 10 min and served as blank for aggregometric study.

Washed platelet preparation by gel filtration

Platelet-rich plasma was isolated by centrifuging fresh human blood, as already described in Platelet preparation section. Apyrase (Sigma, Aldrich, St. Louis, Missouri, USA.) was mixed (0.2 U/mL final concentration) to the isolated PRP to prevent platelet activation and was incubated for 15 min at 37°C. Gel filtered Washed platelet (WP) from PRP was isolated by a 10 mL column of sepharose 2B (Sigma-Aldrich, St. Louis, Missouri, USA.) preequilibrated by the slightly modified Tyrode-Hepes buffer (10 mmol/L HEPES, 137 mmol/L NaCl, 16.8 mmol/L KCl, 2 mmol/L $MgCl_2$, 1 mmol/L $CaCl_2$, 0.119 mmol/L NaHCO3, glucose- 0.1% W/V, pH 7.4). Platelets were eluted in the above-mentioned buffer. The temperature of the buffer was kept at 37°C all along. All steps were carried out under sterile conditions, and precautions were taken to prevent undesirable activation of the platelets as mishandling can cause platelet activation.

Synthesis and isolation of PMP

In vitro synthesis of PMPs was done by activating WP in vitro. For this purpose Chrono-log instrument Model

700 aggregometer, Chrono-log, Havertown, USA, was used. Like standard platelet aggregation process WP was subjected to activation by ADP by a Chrono-log instrument Model 700 with predetermined stirring rate at 1000 rpm for 5 min at 37°C. Final concentration of ADP was 10 μmol/L.

Platelet-derived microparticles synthesized by this process were isolated from the mixture by centrifugation process. The activated mixture was centrifuged at 7000 rpm/4550 *g* by an Eppendorf centrifuge model no 5415R for 5 min at room temperature. The sup containing PMPs was taken out carefully. Platelets having larger size became precipitated by centrifugation.

Loading of NPs and drug into platelet

For this purpose citrate coated iron oxide nanoparticle (FeNP) was used to prepare MON. The FeNP (atomic concentration 173 nmol/L) was synthesized following the method reported in Raja et al. (2010). For loading of drug, fluorescent enabled Doxorubicin hydrochloride (Dox) (from Sigma) a potent anticancer drug, dissolved in filtered Mili-Q water, was used. To loading of NPs and Dox, they were added seperately in the WP (in HEPES buffer) suspension and incubated at 37°C for 1 h in dark (Sarkar et al. 2013). Further experiments were done after that.

Synthesis and isolation of MON and MOD

To synthesize MON, WP were loaded with NP (here we used FeNP). Dox was used to synthesize MOD. In brief, FeNP (final concentration 1.73 nmol/L) and Dox (final concentration 86 nmol/L) was added to the WP seperately and were incubated at 37°C for 1 h at dark. After that, the incubated mixtures were subjected to activation by an Chrono-log instrument Model 700 aggregometer at 37°C with stirring speed 1000 rpm for 5 min Using ADP (final concentration 10 μmol/L) as agonist. FeNP and Dox-loaded PMPs were isolated by centrifugation process.

Loaded PMPs (i.e., MOD and MON) were isolated by centrifuging the mixture at 7000 rpm/4550 *g* for 5 min by an Eppendorf centrifuge model no 5415R at room temperature. By this step, the platelets were pelleted down and the sup-containing MOD or MON were collected carefully and used for further characterization process.

Synthesis and isolation of MOD for in vitro treatment purpose

The isolation procedure of MOD for treatment was very crucial. In brief, Dox (final concentration 86 nmol/L) was incubated with PRP. After 30 min of incubation, Apyrase was added (0.2 U/mL final concentration) to the mixture and incubated for another 30 min. Then the mixture was centrifuged at 326 g for 10 min by an Eppendorf centrifuge model no 5415R and discarded the sup carefully and the pellet was resuspended in complete HEPES buffer. Again Apyrase was added and the process repeated twice. By this free-unloaded Dox was discarded. Then the Dox-loaded platelet suspension was subjected to activation by ADP (final concentration 10 μmol/L) by a Chrono-log instrument Model 700 with predetermined stirring rate at 1000 rpm for 5 min at 37°C. After activation, again the suspension was centrifuged at 7000 rpm/4550 *g* by an Eppendorf centrifuge model no 5415R for 5 min and the sup containing MOD was collected and used for treatment of HeLa cells. All the steps were done in aseptic condition.

CD41 labeling of PMPs

For CD41 labeling, the WP was activated by ADP (final concentration 10 μmol/L) as described earlier. Then PMPs were sorted from the activated WP by BD Aria flow cytometer. Next the sorted MPs were incubated with 20 μL FITC- mouse anti-human CD41 (BD Bioscience) for 60 min at 4°C in dark followed by the addition of an equal amount of 2% paraformaldehyde for 30 min. Then the samples were analyzed by BD Aria flow cytometer (Varon and Shai 2009).

Flow cytometry

Flow cytometry was used to investigate MP production from WP upon ADP activation. In brief, WP was prepared by sepharose 2B coloumn wash from PRP (described in Washed platelet preparation by gel filtration section). Then WP was subjected to activation by ADP (Final concentration of ADP was 10 μmol/L) by a Chrono-log instrument Model 700 with predetermined stirring rate at 1000 rpm for 5 min at 37°C. then the sample was analyzed by a BD Influx flow cytometer taking FSC and SSC in log mode. Only WP served as control here.

Drug loading into the MPs was also characterized by flowcytometry. Briefly, fluorescent enabled Doxorubicin hydrochloride (Dox) (from Sigma) a potent anticancer drug, was incubated with WP at 37°C for 1 h in dark. Then Dox-loaded WP were subjected to activation by ADP in a Chrono-log aggregometer (stated earlier) and MP was isolated by centrifuging the activated mixture at 7000 rpm/4550 *g* by an Eppendorf centrifuge model no 5415R for 5 min at room temperature. The sup containing Dox-loaded MP was taken out carefully. PMPs isolated from only WP served as control (described in Synthesis and isolation of PMP section). Finally the samples were analyzed by a Becton Dickinson Influx flow

cytometer, New Jersey, United States for the presence of fluorescent Dox-loaded MP.

FITC linked CD41 labelled activated PMPs were also analyzed by a Becton Dickinson Influx flow cytometer. The datas were analyzed by either Flow Jo, Tree Star Inc., USA or BD Cell Quest software, New Jersey, United States.

Confocal microscopic study

Slides were prepared for Confocal microscopic examination of MPs for their drug uptake property. In brief, 10 μL of MOD (detailed preparation in Synthesis and isolation of MON and MOD section) was taken in clean and grease free glass slides. Cover slips were then placed on the slides and edges were sealed. The slides were then seen under a laser confocal microscope of Olympus model no IX 81 with FV 1000 software (M/S Olympus Singapore Pte Ltd) and images were captured at 60× magnification with 2.6× optical zoom. From the image of Confocal microscopy, roundedness and feret diameter of the fluorescent red dots was calculated, using Matlab, MathWorks, USA and uthasca Image Tool software (Developed in the Department of Dental Diagnostic Science at The University of Texas Health Science Center, San Antonio, Texas.)

Atomic force microscopic and magnetic force microscopy (Hartmann 1999) study

Atomic Force Microscopic (AFM) study was done to identify the formation of PMPs. In brief, isolated PMPs from activated WP were taken in a cover slip and seen under Nanoscope IV A (Vecco/Digital instruments Innova, Santa Barbara, CA) AFM.

Magnetic Force Microscopic study was done to identify the formation of MON of FeNP. In brief, isolated FeMON (described in Synthesis and isolation of MON and MOD section) was taken in a cover slip. The cover slip was air dried and seen under Nanoscope IV A (Vecco/Digital instruments Innova) AFM in magnetic force microscopy (MFM) mode with different lift height varying from 70 to 500 nm.

Cell culture

Human cervical cancer cell line HeLa and human T lymphocyte cell Jurkat were procured from NCCS, Pune, India. HeLa cell was maintained in DMEM media (Gibco, Thermo Fisher Scientific, USA) supplemented with 10% heat-inactivated fetal bovine serum (Gibco-BRL), 100 U/mL penicillin, 100 μg/mL streptomycin (Gibco-BRL). Jurkat cells were maintained in RPMI media supplemented with 10% heat-inactivated fetal bovine serum (Gibco-BRL), 100 U/mL penicillin, 100 μg/mL streptomycin (Gibco-BRL). The cell lines were treated with MOD and by free Dox at a concentration that equivalent to the concentration of MOD that is, 0.56 nmol/L final concentration. The MOD used for treatment was isolated by the another free-Dox control was made by adding Dox to the MP-treated Hela or Jurkat cells and referred to as MP + Dox control. Another MP control was also prepared in which the cells were treated with only MP. All experiments on the treated cell line were done after 48 h of treatment.

Inverted phase contrast microscopy

HeLa cell was investigated under a phase contrast microscope (eclipse-Ti-U; Nikon, Tokyo, Japan) after treatment for their change in morphology. In brief, 1×10^6/mL HeLa cells were plated in 12 well plate (from NUNC, Thermo Fisher Scientific, USA) and treated with MP_dox (MOD). Only Dox and only MP were also used as the Dox control and MP control, respectively. Untreated HeLa cell was used as control. Another plate was treated by MP and externally added Dox. After 48 h of incubation, the plates were washed by PBS (Gibco-BRL) and seen under microscope using 10× objective lens.

MTT assay

In vitro viability of HeLa cell was determined by 3-[4, 5-dimethylthiazol-2-yl]-2, 5-diphenyltetrazolium bromide (MTT) assay after 48 h of treatment. In brief, cells (1×10^6 cells/mL) were seeded in tissue culture plates (NUNC). After treatment with free Dox, MP, MOD and MP + Dox, MTT (Sigma) solution (final concentration 0.5 mg/mL) was added to each plate and was incubated for additional 4 h at 37°C. Following this, the MTT solution was decanted off carefully and the formazan crystals formed in the viable cells were dissolved in dimethyl sulfoxide. The absorbance was taken at 570 nm with a microplate reader (Biorad, California, USA) (Dong et al. 2015).

Acridine orange – ethidium bromide (AO-EtBr) double staining

Fluorescence microscopy was used to study the entry of AO- EtBr to the treated and untreated Jurkat cells. In brief, cells (1×10^6 cells/mL) were cultured in tissue culture plates (NUNC). After 48 h of treatment with free Dox, MP, MOD and MP + Dox, both treated and untreated Jurkat cells were collected and centrifuged at 1000 rpm for 5 min. The pellet was rinsed twice and resuspended in PBS. The samples were then treated with acridine orange (AO) and ethidium bromide (EtBr) solution (4 μg/mL) and observed under an Olympus (Model no. IX81) fluores-

cence microscope for the qualitative determination of apoptotic cells.

Results

Production and characterization of PMPs

Presence of PMPs were found in the lower FSC and SSC region of Figure 1 when WP was activated with ADP. Figure 1A and B represents dot plot of WP and ADP-activated WP, respectively. The lower FSC- SSC gated population is increased from 22.2% to 59%, which implies production of PMPs. Figure 1C shows the histogram image in which sharp increase in the M1 region after activation of WP by ADP clearly indicates production of PMPs.

To ensure that the produced MPs were derived from platelets, we labelled the activated WP with FITC-conjugated antibody against CD41. Figure 2 shows dot plot with adjacent histogram images of CD41 positive MPs. Figure 2A represents the MP population only. When they are incubated with anti-CD41 antibody, the population shifted toward higher fluorescence (Fig. 2B). Figure 2C represents

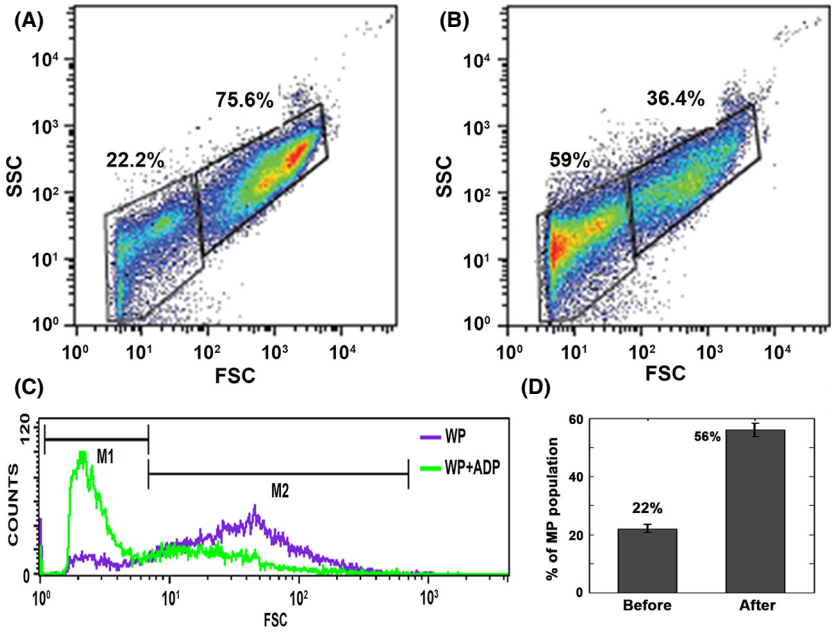

Figure 1. Production of platelet-derived microparticle (PMP) upon ADP activation. (A, B) FSC versus SSC dot plot of washed platelet (WP) (left) and ADP activated WP (right) respectively. (C) Histogram representation of the same. The gated population (M1) is significantly higher when WP was activated by ADP (WP + ADP). (D) Average of microparticle (MP) populations (with error bar) before and after activation of WPs by ADP.

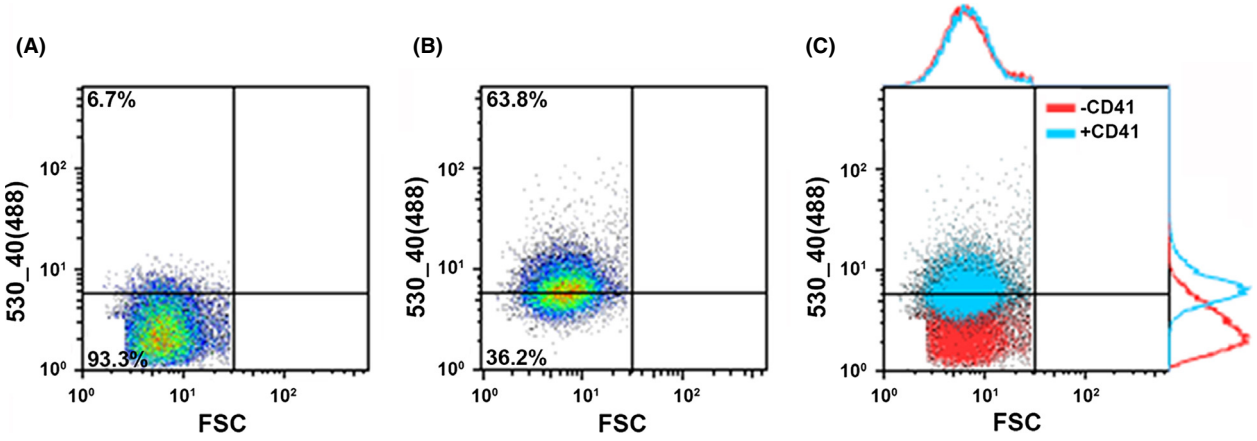

Figure 2. Response to FITC-conjugated anti-CD41 antibody labeling of microparticle. (A) Represents microparticle population from activated washed platelet (WP). (B) CD41 positive population. (C) Overlapping image of A and B with adjacent histogram.

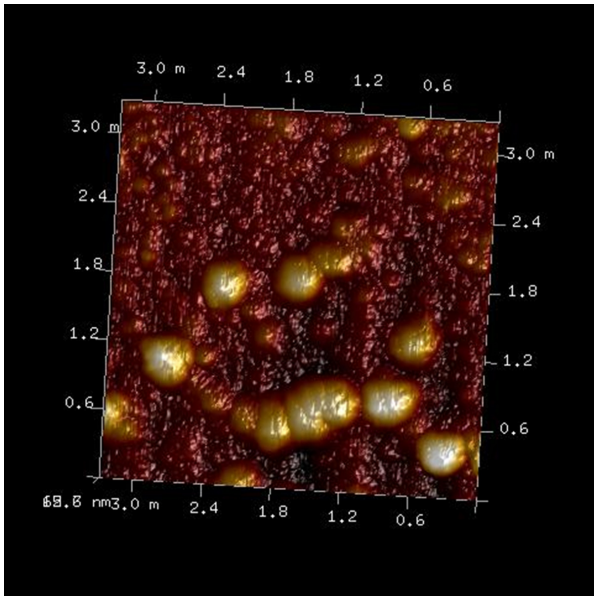

Figure 3. 3D atomic force microscopic (AFM) image of isolated platelet-derived microparticles (PMPs). Surface topology clearly indicates the presence of spherical-shaped PMPs.

the overlapping image of Figure 2A and B with adjacent histogram.

The size of the produced PMPs was obtained from Atomic Force Microscopy (AFM) image. Figure 3 clearly indicates the spherical-shaped MPs with size varying between 300 and 500 nm.

Production of MOD

Doxorubicin hydrochloride (Dox) was used as the model drug for this study. Loading of drug to the PMPs was confirmed by exploiting the fluorescent property of Dox. Figure 4A represents Confocal microscopic image of Dox-loaded PMPs at 60× magnifications with 2.6× optical zoom. Figure 4B demonstrate the roundedness and the feret diameter of the MOD (fluorescent dots), respectively. The upper panel of Figure 4B shows that the fluorescents dot are almost round in shape and their calculated feret diameter was about 200 nm, showed in the lower panel.

Again, flow cytometry also confirms production of drug-loaded MP from loaded platelets. From left to right, Figure 4C demonstrate the FSC- FL2 dot plot profile of isolated PMP from activated WP, MOD and overlap image with adjacent histogram of Figure 4A and B, respectively.

Formation of MON

For this purpose, the iron oxide nanoparticle (FeNP) used here is magnetic in nature and so the prepared MP of FeNP will be magnetic in nature and can be detected by MFM. In Figure 5, the MFM images clearly indicate the presence of magnetically active microparticles with size ranging from 250 to 500 nm. Figure 5A and C are the topological MFM images of each MP of FeNP at 70 and 500 nm lift height, respectively. Figure 5B and D are the corresponding phase image.

Effect of MOD on HeLa cell line

Phase contrast microscopy

Healthier adherent cells maintain their morphology in the culture condition and change in their morphology is characteristic of cytotoxic response. Figure 6 represents phase contrast microscopic images of HeLa cells before and after treatment at lower (10×) magnification. Figure 6A, B, C, D and E respectively represents the phase contrast images of untreated HeLa cell, Dox control (cells treated with Dox solution, corresponding to the concentration of MOD), MP control (cells treated with only MPs), MOD-treated cells and cells treated with MP with external Dox. Notably, the morphology change of MOD-treated HeLa cells is visibly different from other controls.

MTT assay

MTT (3-(4,5-dimethylthiazol-2-yl)-2,5-diphenyltetrazolium bromide) assay has been employed to study the survival rate of the treated and untreated HeLa cells. From Figure 7, it is clear that HeLa cell responds when treated with MOD and showed lower percentage of survival. When treated with free Dox, the percentage of survivability lowered by about 41% compared to the control. But when treated with MOD survivability lowered by about 72% compared to MP control. On the other hand, the effect of free Dox on MP control (MP + Dox control) was not as much as MOD treated. For this case, survivability of HeLa cells was lowered by about 57%.

Double staining

Double staining by AO and EtBr is widely used to differentiate dead cells from live cells. Live cells appear green for AO and dead cells look orange for EtBr due to loss of membrane integrity. Figure 8 is the merged microscopic image of green and red filter of double-stained-treated and untreated jurkat cells. From left to right, the images represent control, Dox control, MP control, MOD treated and MP + Dox-treated cells, respectively. From Figure 8 it is clear that the number of live cells markedly decreases

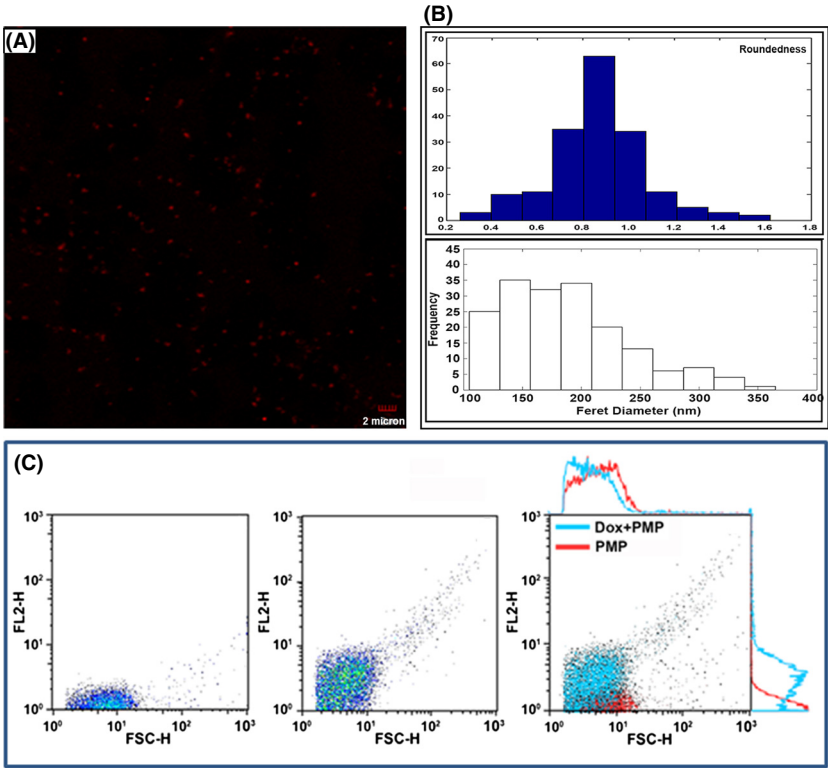

Figure 4. (A) Confocal microscopic image of Dox-loaded microparticles (MOD) at 60× magnifications with 2.6× optical zoom with scale bar of 2 μm. (B) Upper panel and lower panel represents the roundedness and feret diameter. (C) Left and middle panel shows the dot plot of platelet-derived microparticles (PMPs) and MOD. Right panel is the overlapping image of the left and middle panel. MOD, microparticle of drug.

in MOD-treated (Dox-loaded MP) Jurkat cells compared to any other set. Presence of apoptotic body in this group suggests that cell death occurs via apoptosis.

Discussion and Conclusion

The paper reveals two independent perspectives related to MPs. Microparticles in the clinical regime are used as markers. In the material science context MPs are normally synthesized in the solid phase route. In our case, we have used a wet route to synthesize MP and we have shown how it can be effectively used as a drug carrier and also as a material containing nanocomposite. While we have used platelets as a source of MPs, alternative sources of the same can also be exploited for the said purpose. The platelet, however, has an advantage. Whole platelets incidentally can also be used as drug carrier (Sarkar et al. 2013).

Platelets are terminally differentiated cells unable to undergo cellular division. After they are released from cytoplasm of megakaryocytes to blood stream, it is possible to identify them in the peripheral blood by assessing membrane glycoprotein receptors such as GPIIb (CD41), GPIbα (CD42), GPIIIa (CD61) and others (Metcalfe et al. 2003; Patel et al. 2005). Upon activation, platelets shed membrane components containing certain membrane receptors and other proteins inherited from parental cells. These components are called PMPs or platelets-derived microvesicles. These vesicles are in between, 80 and 400 nm in diameter and carry surface molecules that are typical for the cell that releases them (György et al. 2011; Distler et al. 2005).

We have synthesized and isolated MPs from platelets in vitro. Upon activation with ADP, WP produces MPs that are detected in the low FSC-SSC region (Fig. 1) of dot plot. Production of MPs before activation by ADP is minimal and the activation is realized only after addition of the agonist ADP. Thus is clearly documentaed in the Table 1 of the supplementary section. The unpaired *t*-test also shows that there is significant higher activation only after agonist addition.The size of this MPs are between 300 and 500 nm and spherical in shape. This is shown by atomic force microscopy (Fig. 3). The MPs produced by this process harbor CD41 (Fig. 2), a characteristics surface marker of platelet. In addition, the MPs are CD62P positive (see Fig. S4) this being an activation marker of platelets.

It may be note that this is the first report of loading MP with an anticancer drug using a simple biocatalytic

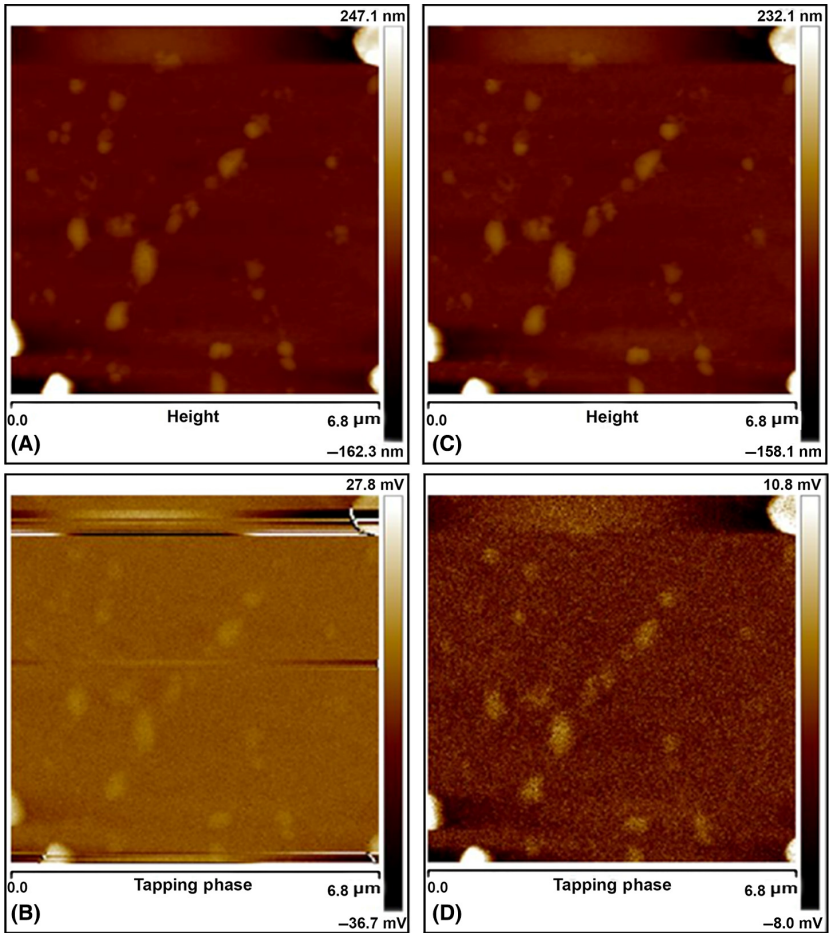

Figure 5. Magnetic force microscopy (MFM) image of FeMON. (A) and (C) are the topological image of FeMON at 70 and 500 nm lift height respectively. Image (B) and (D) are the corresponding phase image.

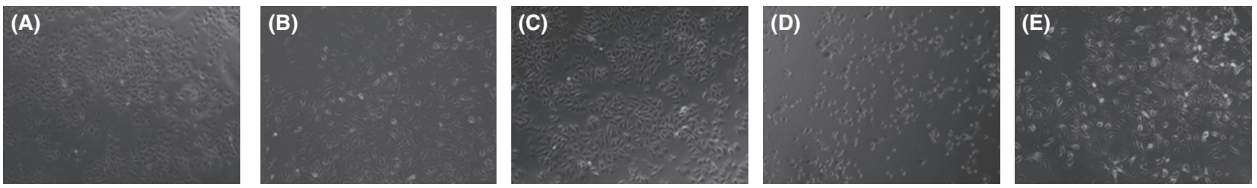

Figure 6. Phase contrast microscopic images of untreated (A), free Dox treated (B), MP treated (C), MOD treated (D) and MP with free Dox-treated (E) HeLa cells, respectively. MOD, microparticle of drug; MP, microparticle.

route, namely the platelet activation. Drug-loaded platelets when subjected to activation by agonist secrete MPs loaded with drug (Fig. 4) 3D reconstituted confocal image of Dox-loaded platelets (data not shown) reveals that platelets internalize Dox to their inner cellular millue. As MPs harbor cell-surface proteins and contain cytoplasmic components of their parental cells (Li and Cong 2009), so, activated drug-loaded platelets secrete drug-loaded MPs. Incidentally, the drug uptake process is proportional to the applied drug concentration (see Figs. S1, S2).

We intended to extend the said approach for loading NPs (instead of drugs). This will enable a smart NP to be easiliy internalized in the cell. We have confirmed that such loading is possible using a magnetic nanoparticle (FeNP) (Raja et al. 2010) and the fact that it retains the magnetic property of the NP is evident from the magnetic force microscopic image (Fig. 5). We must again mention

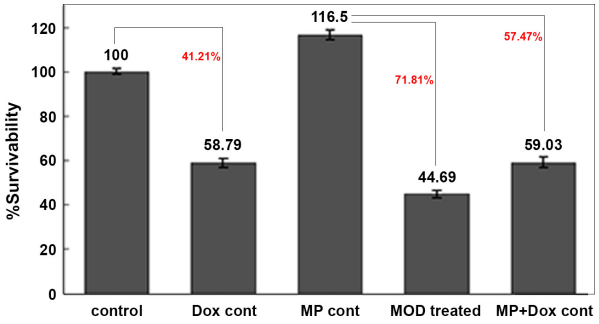

Figure 7. Cell viability of untreated, free Dox-treated, MP treated, MOD treated and MP with free Dox-treated HeLa cells respectively. MOD, microparticle of drug; MP, microparticle.

that this route of loading NP in the MPs is novel. Microparticles synthesized from FeNP-loaded platelets show the magnetic property and thus detected by MFM. The stricking aspect is that even at 500 nm lift height, at which the vander Waal forces are insignificant (Fig. 5D), the MP can be detected. The size of the objects found in MFM (Fig. 5) correlates with the size of the PMPs found in the AFM (Fig. 3).

We again assert that the MP-loaded drug has a higher potential than the free drug in imaprting cytotoxicity to cancer cells and if any nanoparticle-conjugated drug is available the micropatricles can serve as secondary carriers for the said purpose. The Table 2 of supplementary clearly shows the higher potential of the MPs and the ratio of the percentage survival after and before treatment has the lowest value in case of MP-loaded drug as compare to other controls like only drug and MP and drug added seperately.

As derived from platelets, the MPs harbor the surface receptor molecules those are capable of interacting with cancer cells as their perental cells that is, platelets (Mezouar et al. 2014). The suggestion of using MPs as drug delivery vehicle comes from the results of our in vitro experiments. We have successfully loaded PMPs with Doxorubicin hydrochloride, a potent anti-cancer drug (Fig. 4). In phase contrast microscopy and cell viability assay (Figs. 6, 7), it was observed that the cytotoxicity of

Table 1. Microparticle (MP) release by ADP addition in washed platelets.

	% MP	
No. expt	Active before ADP addition	Active after ADP addition
1	22.3	59
2	21	52.9
3	24	55
4	21.1	57.1

P-value rejecting the null hypothesis ($H = 0$) = 4.7×10^{-7} at confidence level 99.9%.

Table 2. Survival ratio after and before the treatment.

	Treatment		
	DOX	MP_DOX	MP + DOX
#1	0.59	0.37	0.52
#2	0.57	0.38	0.48
#3	0.59	0.38	0.50
t-stat	–	$H = 1$, $P = 6.4 \times 10^{-4}$, at confidence level 99.9%	
t-stat	$H = 1$, $P = 5.1 \times 10^{-6}$, at confidence level 99.9%		–

MOD is visibly higher than any other controls used to treat HeLa cells. HeLa, human cervical cancer cell line, was used as a model cancer cell. From the experiments it was observed that MP alone can boost the cell growth and thus viability of HeLa cells increases (Fig. 7). This is because due to the growth factors provided by the PMPs. That's why we compared the cytotoxicity effect of MOD with MP and free Dox-treated cells (MP + Dox cont of Fig. 7), but not with only free Dox-treated cells (Dox cont of Fig. 7). Dose of free Dox was calculated by the standard curve of Dox (Fig. S3). Phase contrast microscopy also provides similar results (Fig. 6). HeLa cell morphology altered significantly by the effect of MOD.

The results of Live/dead assay also support the previous results (Fig. 8). Jurkat cells exert more cytotoxicity after treatment with Dox-loaded microparticles (MOD)

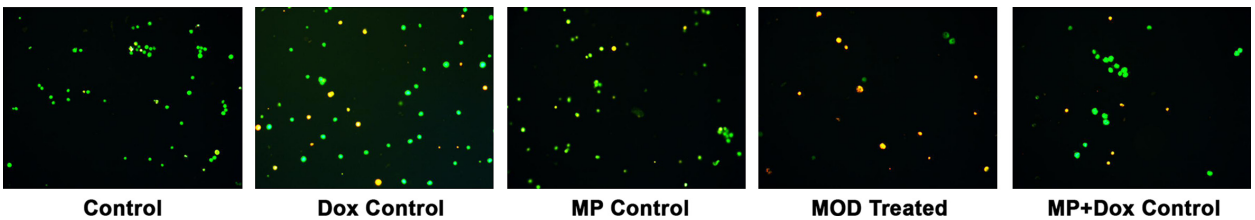

Figure 8. Acridine orange/EtBr double staining of Jurkat cells. From left to right, the images represent control (untreated), free Dox-treated, only MP-treated, MOD-treated and MP + Dox (MP with free Dox)-treated cells, respectively. MOD, microparticle of drug; MP, microparticle.

compared to any other group of treatment. Statistical analysis by Matlab software of the images of live/dead cells assay reveals more than 85% of MOD-treated Jurkat cells are susceptible to EtBr, wheareas other groups are below 40% (analysis not shown). So, Phase contrast microscopy MTT assay and live/dead cells assay, imply, MPs as the promising drug delivery vehicles.

Not only in the field of drug delivery, the study may be open the door in the field of bio imaging to diagnosis by using MONs as constituent NP (say quantum dots) can help such imaging (or flow cytometric analysis).

In this study we have designed MPs exploiting thrombotic property of platelets suitable for efficient drug delivery. The MPs are intrinsically biocompatible and devoid of immune response. The advantage of the method is that it is readily detected by simple methods like flow cytometry, confocal microscopy. The model drug Dox remains significantly active at concentration at which free drug remains practically inactive. Furthermore the biological route can be exploited to preapare MPs composed of NPs that may irrespective of their colloidal properties. As example, a magnetic MP is produced by assembliing FeNPs, using the thrombotic route. Lastly, we may say that the proposed method of MPs from drugs and NPs may be of significant future phrmaceutical interest.

Acknowledgements

We acknowledge ICMR, India (Grant no. 45/06/2011/NAN-BMS) for supporting the research. We thank Puja Biswas and Bonny Halder of DBT- IPLS of Calcutta University for assistance in the AFM and Confocal Microscopy.

Disclosures

The authors do not have any conflict of interest.

References

Alagusundaram M, Umashankari K, Badarinath AV, Lavanya C, Ramkanth S (2009). Microspheres as a novel drug delivery sysytem-a review. Int J Chemtech Res 1: 526–534.

Bastarache JA, Fremont RD, Kropski JA, Bossert FR, Ware LB (2009). Procoagulant alveolar microparticles in the lungs of patients with acute respiratory distress syndrome. Am J Physiol Lung Cell Mol Physiol 297: L1035–L1041.

Berckmans RJ, Nieuwland R, Böing AN, Romijn FP, Hack CE, Sturk A (2001). Cell-derived microparticles circulate in healthy humans and support low grade thrombin generation. Thromb Haemost 85: 639–646.

Burnier L, Fontana P, Kwak BR, Angelillo-Scherrer A (2009). Cell-derived microparticles in haemostasis and vascular medicine. Thromb Haemost 101: 439–451.

Chandler W, Yeung W, Tait J (2011). A new microparticle size calibration standard for use in measuring smaller microparticles using a new flow cytometer. J Thromb Haemost 9: 1216–1224.

Cocucci E, Racchetti G, Meldolesi J (2009). Shedding microvesicles: artefacts no more. Trends Cell Biol 19: 43–51.

Cook E, Stahl J, Lowe L, Chen R, Morgan E, Wilson J, et al. (2001). Simultaneous measurement of six cytokines in a single sample of human tears using microparticle-based flow cytometry: allergics vs. non-allergics. J Immunol Methods 254: 109–118.

Copple IM, Goldring CE, Kitteringham NR, Park BK (2008). The Nrf2–Keap1 defence pathway: role in protection against drug-induced toxicity. Toxicology 246: 24–33.

Dastjerdi R, Montazer M (2010). A review on the application of inorganic nano-structured materials in the modification of textiles: focus on anti-microbial properties. Colloids Surf B 79: 5–18.

Davila M, Amirkhosravi A, Coll E, Desai H, Robles L, Colon J, et al. (2008). Tissue factor-bearing microparticles derived from tumor cells: impact on coagulation activation. J Thromb Haemost 6: 1517–1524.

Distler JH, Jüngel A, Huber LC, Seemayer CA, Reich CF, Gay RE, et al. (2005). The induction of matrix metalloproteinase and cytokine expression in synovial fibroblasts stimulated with immune cell microparticles. Proc Natl Acad Sci USA 102: 2892–2897.

Dong L, Li M, Zhang S, Li J, Shen G, Tu Y, et al. (2015). Cytotoxicity of BSA-stabilized gold nanoclusters: in vitro and in vivo study. Small 11: 2571–2581.

Enjeti AK, Seldon M (2012). Microparticles: role in haemostasis and venous thromboembolism. May ed. INTECH Open Access Publisher, Croatia.

Guo J, Yang W, Wang C, He J, Chen J (2006). Poly (*N*-isopropylacrylamide)-coated luminescent/magnetic silica microspheres: preparation, characterization, and biomedical applications. Chem Mater 18: 5554–5562.

Hartmann U (1999). Magnetic force microscopy. Annu Rev Mater Sci 29: 53–87.

Horstman LL, Ahn YS (1999). Platelet microparticles: a wide-angle perspective. Crit Rev Oncol Hematol 30: 111–142.

Joop K, Berckmans RJ, Nieuwland R, Berkhout J, Romijn FP, Hack CE, et al. (2001). Microparticles from patients with multiple organ dysfunction syndrome and sepsis support coagulation through multiple mechanisms. Thromb Haemost 85: 810–820.

Jyothi NVN, Prasanna PM, Sakarkar SN, Prabha KS, Ramaiah PS, Srawan G (2010). Microencapsulation techniques, factors influencing encapsulation efficiency. J Microencapsul 27: 187–197.

Kahaleh M, Mishra R, Shami VM, Northup PG, Berg CL, Bashlor P, et al. (2008). Unresectable cholangiocarcinoma: comparison of survival in biliary stenting alone versus stenting with photodynamic therapy. Clin Gastroenterol Hepatol 6: 290–297.

Kang L, Chung BG, Langer R, Khademhosseini A (2008). Microfluidics for drug discovery and development: from target selection to product lifecycle management. Drug Discovery Today 13: 1–13.

Lee SC, Oh JT, Jang MH, Chung SI (1999). Quantitative analysis of polyvinyl alcohol on the surface of poly (D, L-lactide-co-glycolide) microparticles prepared by solvent evaporation method: effect of particle size and PVA concentration. J Controlled Release 59: 123–132.

Li X, Cong H (2009). Platelet-derived microparticles and the potential of glycoprotein IIb/IIIa antagonists in treating acute coronary syndrome. Tex Heart Inst J 36: 134.

Matyjasik-Liggett M, Wittman P (2013). The utilization of occupational therapy services for persons with Charcot-Marie-Tooth disease. Occup Ther Health Care 27: 228–237.

Metcalfe P, Watkins N, Ouwehand W, Kaplan C, Newman P, Kekomaki R, et al. (2003). Nomenclature of human platelet antigens. Vox Sang 85: 240–245.

Mezouar S, Mege D, Darbousset R, Farge D, Debourdeau P, Dignat-George F (2014). Involvement of platelet-derived microparticles in tumor progression and thrombosis. Seminars in oncology. Elsevier 41: 346–358.

Mu L, Feng S (2001). Fabrication, characterization and in vitro release of paclitaxel (Taxol®) loaded poly (lactic-co-glycolic acid) microspheres prepared by spray drying technique with lipid/cholesterol emulsifiers. J Controlled Release 76: 239–254.

Padalkar AN, Shahi SR, Thube MW (2011). Microparticles: an approach for betterment of drug delivery system. IJPRD 3: article no. 12.

Patel SR, Hartwig JH, Italiano JE Jr (2005). The biogenesis of platelets from megakaryocyte proplatelets. J Clin Invest 115: 3348.

Raja SO, Chaudhuri RK, De R, Dasgupta AK (2010). Ferritin biosensor and methods of using the same: Google Patents.

Ramachandraiah K, Han SG, Chin KB (2015). Nanotechnology in meat processing and packaging: potential applications – a review. Asian-Australas J Anim Sci 28: 290–302.

Rejman J, Oberle V, Zuhorn I, Hoekstra D (2004). Size-dependent internalization of particles via the pathways of clathrin-and caveolae-mediated endocytosis. Biochem J 377: 159–169.

Sarkar S, Alam MA, Shaw J, Dasgupta AK (2013). Drug delivery using platelet cancer cell interaction. Pharm Res 30: 2785–2794.

Schindler SM, Little JP, Klegeris A (2014). Microparticles: a new perspective in central nervous system disorders. BioMed Res Int 2014: 756327–756344.

György B, Módos K, Pállinger É, Pálóczi K, Pásztói M, Misják P et al. (2011). Detection and isolation of cell-derived microparticles are compromised by protein complexes resulting from shared biophysical parameters. Blood 117: e39–e48.

Varon D, Shai E (2009). Role of platelet-derived microparticles in angiogenesis and tumor progression. Discov Med 8: 237–241.

Yeo Y, Baek N, Park K (2001). Microencapsulation methods for delivery of protein drugs. Biotechnol Bioprocess Eng 6: 213–230.

Supporting Information

Additional Supporting Information may be found in the online version of this article:

Appendix S1. Microparticle syntheis profile (Figures S1 & S2) standard curve showing fluorescence increase with Dox concentration (Figure S3) and microparticle isolation by different methods.

Figure S1. Histogram peak of MPs synthesized when WP was incubated with 86 nmol/L (blue line), 129 nmol/L (saffron line) and 172 nmol/L (green line).

Figure S2. *X* axis represents the amount of Dox applied to the platelets. *Y* axis represents the bulk concentration of Dox loaded to the MPs.

Figure S3. Standard curve of Doxorubicin Hydrochloride (Dox).

Figure S4. FITC-CD62P labeling of PMPs isolated by centrifugation process and flow cytometric sorting method.